# UAV-BASED REMOTE SENSING OF LANDSLIDES

U. Niethammer [a], S. Rothmund [a], M. R. James [b], J. Travelletti [c], M. Joswig [a]

[a] Institute for Geophysics, Universität Stuttgart, 70174 Stuttgart, Germany - uwe.niethammer@geophys.uni-stuttgart.de
[b] Lancaster Environment Centre, Lancaster University, Lancaster, UK - m.james@lancaster.ac.uk
[c] School and Observatory of Earth Science, University of Strasbourg, France - julien.travelletti@eost.u-strasbg.fr

**KEY WORDS:** UAV, Quad-rotor, Landslide, Photogrammetry, DEM, DSM

**ABSTRACT:**

In this study a low-cost remote sensing approach based on unmanned aerial vehicles (UAVs) and digital compact cameras will be presented. This approach enables high-resolution acquisitions of landslides. The concept of manual controlled quad-rotor helicopters has been investigated for photogrammetric applications, since quad-rotor systems have been proved to be well suited for landslide monitoring in difficult alpine terrain. During the UAV-based remote sensing campaigns significant numbers of airborne photographs of the Super-Sauze landslide (Southern France) have been acquired. These photographs were combined to an ortho-mosaic by applying plane image rectification methods. Digital surface models (DSMs) were generated using a new feature-based surface reconstruction approach which does not require any ground control point information.

## 1. INTRODUCTION

### 1.1 Study area

This study was carried out on the Super-Sauze landslide (Southern French Alps). The Super-Sauze landslide is located on the North-facing slope of the Barcelonnette Basin. It has developed in a torrential basin located in the upper part of Sauze torrent. The landslide is one of the persistently active landslides (since the 1970's). It extends over a horizontal distance of 850 m and occurs between an elevation of 2105 m at the crown and 1740 m at the toe with an average of 25° slope. Its total volume is estimated to be 750.000 m³ and velocities range from 0.01 m up to 0.4 m per day (Malet et al. 2003).


Figure 1. Super-Sauze landslide

### 1.2 Previous UAV-based remote sensing

UAV-based remote sensing studies have been carried out for many decades. In the late 1970's fixed wing remote controlled aircrafts have been investigated for first motorized UAV photogrammetry experiments (Przybilla and Wester-Ebbinghhaus, 1979). A quarter century later Eisenbeiss et al. (2005) generated the first high-resolution digital elevation models (DEMs) using autonomously controlled helicopter UAVs. Today there are many other UAV-systems like motorized paragliders (Jütte, 2008), blimps (Gomez-Lahoz and Gonzalez-Aguilera, 2009), kites (Aber et al., 2002) and balloons (Fotinopoulos, 2004) in use. But such systems are strongly affected by wind and often cannot be used in alpine terrain. Since 2006 quad-rotor systems are available as open source projects (Mikrokopter, 2009). When compared to commercially available UAV-systems, the costs of such open source systems are very low and all software source codes, as well as electronic schematics are available in the public domain.

### 1.3 UAV-based remote sensing in landslide research

Monitoring and analysis of active landslides involves both spatial and temporal measurements and requires continued assessment of landslide conditions, including the extent and rate of displacements as well as changes in the surface topography. Displacement rates are of great interest and can be directly achieved by the comparison of ortho-photographs as well as digital surface models (DSMs) from different dates. Such measurements can be performed manually or automatically, for example by image correlation algorithms (Leprince et al., 2008). UAV-acquired ortho-mosaics now allow for a detailed large scaled analysis of landslide materials and fissure structures (Walter et al., 2009). Such fissure structures have been clearly detected and could be related to fracture processes in the landslide material. Additionally, high-resolution textural information in UAV-acquired ortho-photographs could possibly permit a soil moisture analysis of the surface of landslides (Niethammer et al., 2009). Such analysis could be supported by multi-spectral analysis in the near- and thermal infrared spectrum. One major advantage of UAV-based remote sensing applications for hazardous environments like landslides, mudslides or rockfalls is the possibility to gain information in very dangerous areas of interest. Direct measurements in such area often are impossible.

### 1.4 UAV-based photogrammetry

Up to now UAV-based photogrammetric evaluations are still very difficult. UAV-acquired airborne photographs are required to be in an optimal block configuration alignment in order to manage standard aerial photogrammetric processing. In addition the camera-systems are required to maintain a stable interior orientation, as well as reduced optical distortions and a lightweight but robust design. These requirements have been solved in the past by the usage of high-end fixed-lens SLR-cameras, as well as precise UAV navigation based on high-end autopilot- and UAV-systems and special developed photogrammetric software packages (Eisenbeiss et al., 2005).

Here we present a low-cost UAV-based remote sensing approach using new structure from motion algorithms which can reduce limitations when using manual controlled UAVs and digital low-cost compact cameras. These methods easily can handle unordered image collections and do not require any ground control point information. Therefore this approach is very suitable in the field of landslide research.

## 2. UAV-SYSTEM

### 2.1 Quad-rotor UAV

When compared to conventional helicopters, quad-rotor systems are more stable in flight with reduced vibration and have the mechanical advantage of not requiring a large, variable pitch rotor-unit. Our in-house developed quad-rotor system is stabilized by inertial measurement units (IMU), including three acceleration sensors, three gyroscopes, a three-axis compass, a pressure sensor, and is regulated by basic PID (proportional integral differential) loops. A quad-rotor open source project (Mikrokopter, 2009) has been used and improved by modifications of the software and the electronic circuit in order to comply with the requirements for landslide studies.


Figure 2. Modified Mikrokopter-system

### 2.2 Autonomous versus manual flight

Autonomously controlled UAVs have been proved to be successful for first remote sensing applications but they do not benefit from the intelligence of a human operator and, currently, are less able to cope with unpredictable conditions such as gusty winds. In addition, the use of autonomously controlled UAVs is tightly regulated by civil aviation and security authorities, preventing their practical deployment.

In this study radio-controlled UAVs have been used. This requires a good level of pilot skill, and range restrictions limit the operational area to a few hundreds of meters. There are also further issues related to the relatively small payloads and UAV-reliability. However, the advantages of using manual controlled quad-rotor UAVs currently are significant.

### 2.3 Camera-system

The quad-rotor UAVs are equipped with lightweight low-cost digital compact cameras, which support manual camera settings. For all flights the camera settings were fixed to ISO 200 at F2.8 and a focus of 6.2 mm. These settings enabled an average shutter speed of 1/800 s which was necessary to avoid blurred photographs.


| | |
|---|---|
| sensor size | 1 / 2.5" |
| resolution | 3264 x 2448 |
| lens | F2.8 to F5.2 |
| focus | 6.2 mm – 16.6 mm |
| shutter speed | 1 / 2000 s |
| sensitivity | ISO 50 – ISO 1600 |
| weight | 110 g |
| price | 100 € |

Figure 3. UAV camera-system

## 3. IMAGE ACQUISITION

In October 2008 a set of 1486 UAV-acquired photographs covering the whole sliding area of 850 m x 250 m were taken. The achievable altitude over ground was in the range between 20 m and 250 m. All photographs were taken in an automatic image series mode shooting one photo every three seconds. In a first in-situ flight planning step, the desired area and suitable locations for starting and landing were chosen. Then the quad-rotor was launched to the maximum flight altitude of about 200 m. At this position the UAV was hovered for about 30 seconds. Vertical landing was then initiated by the pilot. After each flight the covered area of the acquired photographs was checked on the camera directly.

## 4. DIGITAL SURFACE MODEL PROCESSING

The field of computer vision now offers methods for extraction of 3D surface models from overlapping digital images as an efficient alternative to commercial photogrammetry software. Immense progress has been made on algorithms for multiple view reconstruction. Such multi view stereo (MVS) algorithms are now robust and accurate and do not require any ground control point information or tie points as usually required for standard photogrammetric processing. Additionally, an optimized initial block alignment for the photogrammetric processing is not required.

The proposed MVS method consists of a structure from motion algorithm (Snavely et al., 2008) for automated camera calibration and bundle block computation, as well as a patch based multi view stereo algorithm for the generation of dense 3D point cloud models (Furukawa and Ponce, 2007).

### 4.1 Structure from motion algorithm

The structure from motion algorithm (Snavely et al., 2008) computes a set of parameters for each of the supplied photographs (extrinsic and intrinsic camera parameters, as well as a sparse 3D point cloud). It does not rely on a previous camera calibration or any other information to provide location, orientation, or geometry. Instead this information is computed from the images themselves. For all images, SIFT key-point descriptors (Lowe, 2004) are matched, using an approximate nearest neighbour algorithm (ANN) (Arya et al., 1998). After matching features a robust fundamental matrix is estimated for each image pair using the RANSAC algorithm (Fischler and Bolles, 1981). Finally a set of camera parameters and the relative 3D locations between all supplied images is calculated (e.g. rotation, translation, focal length and radial distortion parameters), as well as a new set of undistorted photographs.

### 4.2 Patch-based multi view stereo algorithm

The patch-based multi view stereo algorithm (Furukawa and Ponce, 2007) computes a dense set of small rectangular patches covering the surfaces visible in the images using the supplied parameters from the structure from motion algorithm. Stereopsis is implemented as a match, expand, and filter procedure, starting from a sparse set of matched key points, and repeatedly expanding these before using visibility constraints to filter away false matches. The keys to the performance of the algorithm are effective techniques for enforcing local photometric consistency and global visibility constraints.

### 4.3 Alignment adjustment of the point cloud

Since the investigated algorithms do not consider any ground control point information the coordinate system of the final 3D point cloud remains indeterminate. This is the major disadvantage of this approach, but can be solved applying a spatial similarity transformation to all points of the computed 3D model:

$$X_t = T + sRX \quad (1)$$

where $X_t$ = transformed coordinate vector
$X$ = initial coordinate vector
$T$ = translation vector
$R$ = rotation matrix including $r_x$, $r_y$, $r_z$
$r_x$, $r_y$, $r_z$ = rotations around the coordinate axes
$s$ = scale factor

Seven parameters are required for this kind of transformation and were calculated from a set of three well known prominent locations which were visible in a computed hillshading of the generated point cloud. However, this strategy is susceptible to misalignments of the final DSM, because of the limited precision possible when registering ground control points using only a shaded relief model.

### 4.4 Processing

30 photographs of the landslide toe-region, as well as 285 photographs of the entire landslide (manually pre-selected by criteria like image quality and covered area size) were computed to two digital surface models, one of the toe and one of the entire landslide.
First, all photographs were processed using the structure from motion algorithm. This computation supplied a set of camera parameters and the relative 3D locations between all supplied images, as well as a new set of undistorted images. In a second step these data were supplied to the patch based multi view stereo algorithm which finally computed a dense point cloud for all supplied photographs.

### 4.5 Ortho-mosaic computation

Since the proposed photogrammetric methods do not directly generate an ortho-mosaic, a straightforward plane image rectification method as described in Niethammer et al. (2009) has also been used (figure 9). In a first step, optical barrel distortion of the camera was corrected. In a second processing step, each image was rectified manually onto DGPS-measured ground control point (GCP) coordinates using plane image rectification approaches. In a final step all rectified photographs with a ground resolution in the range of 3 to 8 cm have been merged to a high-resolution ortho-mosaic. However, this approach requires a significant amount of manual processing and the presence of residual misalignments has to be accepted.

### 4.6 DSM precision analysis

In order to assess the quality of the generated digital surface models, the surface model of the landslide toe-region (figure 4) was compared to the result of a previously performed photogrammetric investigation (James et al., 2010) (figure 5) using a GOTCHA region-growing algorithm (Otto and Chau, 1989). Both surface reconstructions were computed using the same photographs.

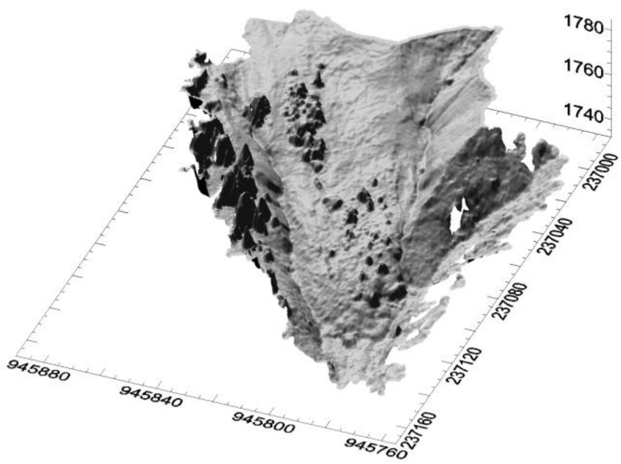


Figure 4. DSM for precision analysis of the toe region, generated using the proposed MVS algorithms

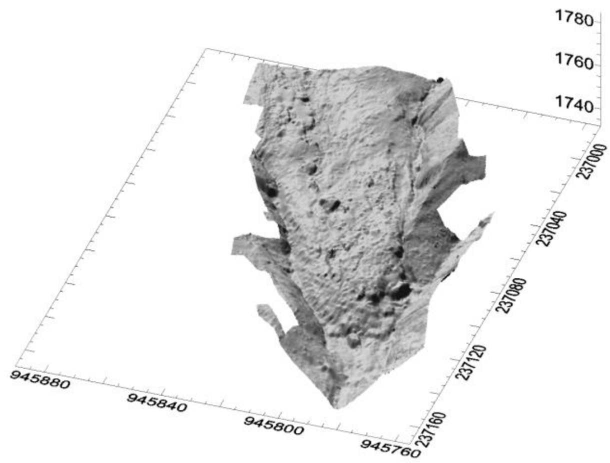


Figure 5. DEM of the toe region, generated using a GOTCHA region growing algorithm (James et al., 2010)

The surface model of our proposed method (figure 4) shows a little denser point cloud (figure 6B) compared to the other model (figure 6A), especially in the middle part of the investigated area.

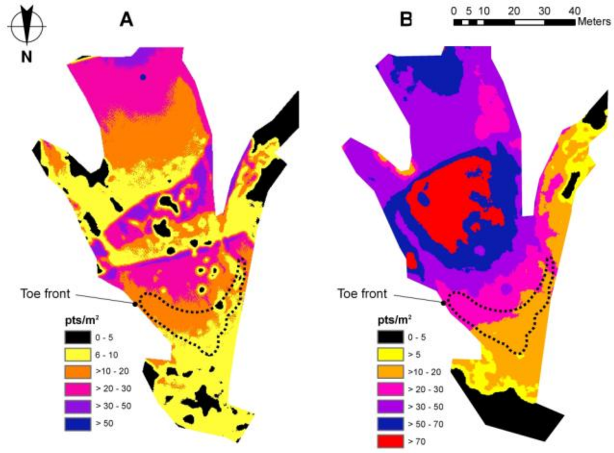


Figure 6. Comparison of the point density. A: DEM generated using a GOTCHA region-growing algorithm. B: DSM generated using the proposed MVS approach.

In figure 8 the point density of the surface model of the entire landslide is illustrated. Some sparse areas can be observed (illustrated by yellow and white) as a result of supplying too few photographs of this areas to the algorithms. Additionally an analysis of the alignment was done by subtracting the elevation of both models of the toe-region (figure 7). In the vertical direction deviations reach from -3 m to +4 m. These significant deviations reflect the presence of vegetation which was removed in only one of the investigated models (figure 5). Further sizable differences of about one meter from north to south direction can be observed. These differences can be explained by misalignments when using a shaded relief for the registration of the GCPs and it is anticipated that they can be significantly reduced in further work. In general it can be concluded that both photo-based methods provide consistent surface models.

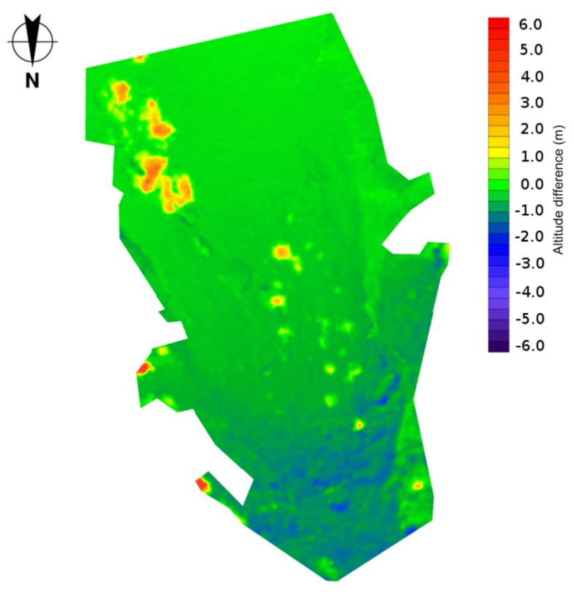


Figure 7. Altitude differences between the GOTCHA- and the MVS-generated DEM of the toe-region

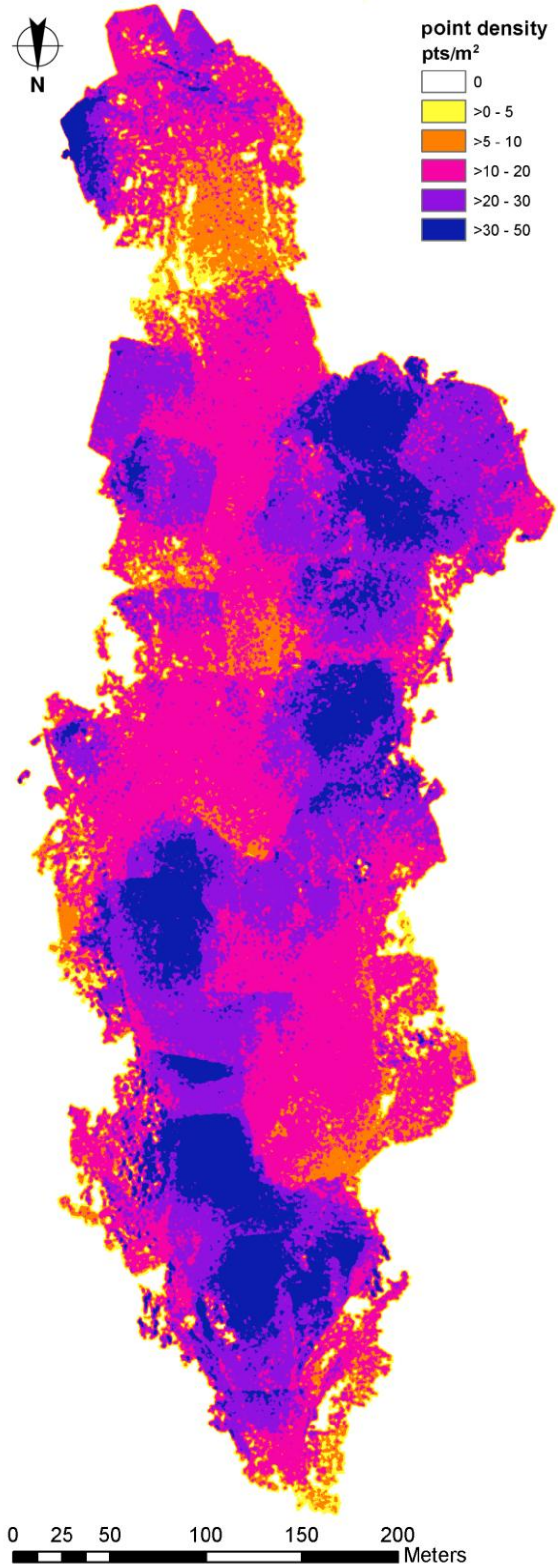


Figure 8. Point density of the entire landslide surface model

## 5. RESULTS

In figure 9 an ortho-mosaic of the Super-Sauze landslide is illustrated. Figure 10 shows a hillshading of the generated digital surface model. These results are showing a good agreement and are suitable for high-resolution investigations of the entire Super-Sauze landslide.

### 5.1 Resulting ortho-mosaic

59 UAV-acquired photographs have been merged to an ortho-mosaic by using plane image rectification methods. The generated ortho-mosaic covers the entire sliding area of the Super-Sauze landslide (figure 9), with a spatial resolution in the range of 3 cm to 8 cm. Within the ortho-mosaic some misalignments are present. The maximum deviation within the boundary of the sliding area reaches 3.9 m and the mean error can be quantified to be 0.5 m.

### 5.2 Resulting digital surface model

285 pre-selected photographs were computed to a digital surface model of the entire landslide. The point density of the achieved model varies between 0 and 40 points per square meter. A grid size of 30 cm was chosen in order to avoid interpolation artefacts in sparse areas of the point cloud (the maximum point density would allow a grid size of 20 cm). The achieved digital surface model shows clearly the details of the shape of the landslide but a misalignment up to several meters is present.

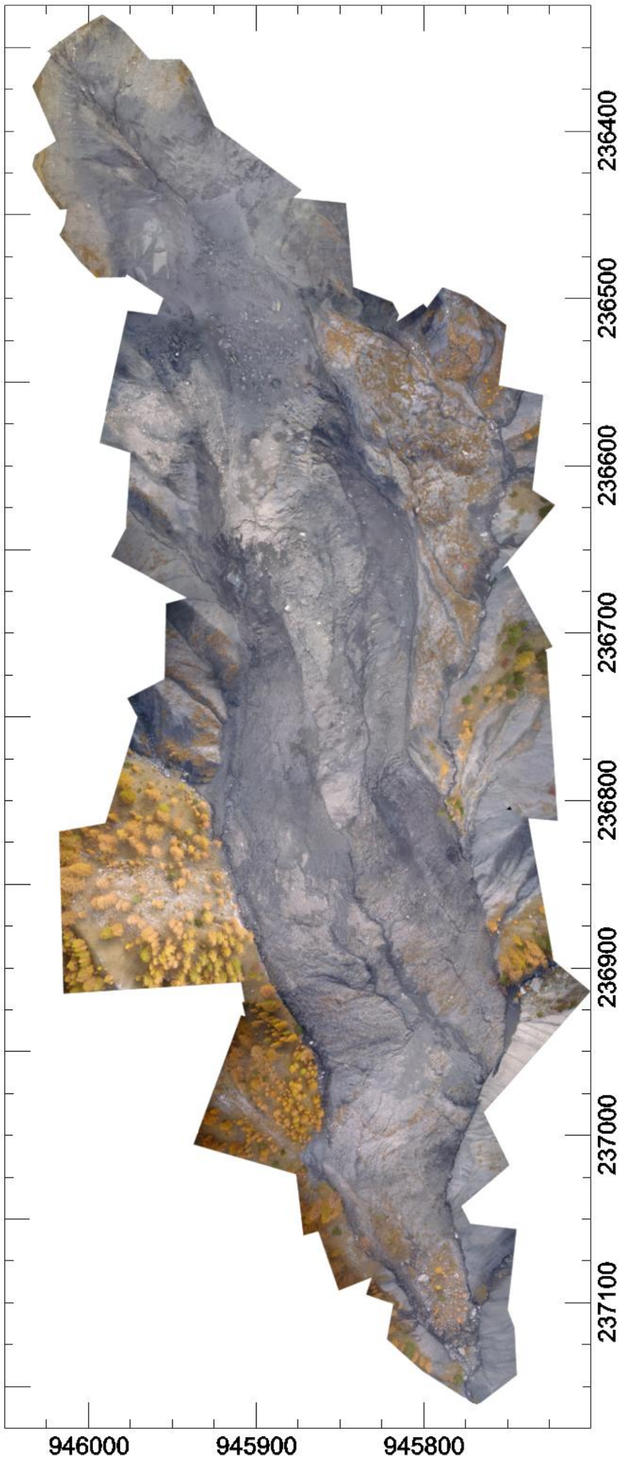


Figure 9. Ortho-mosaic of the entire Super-Sauze landslide

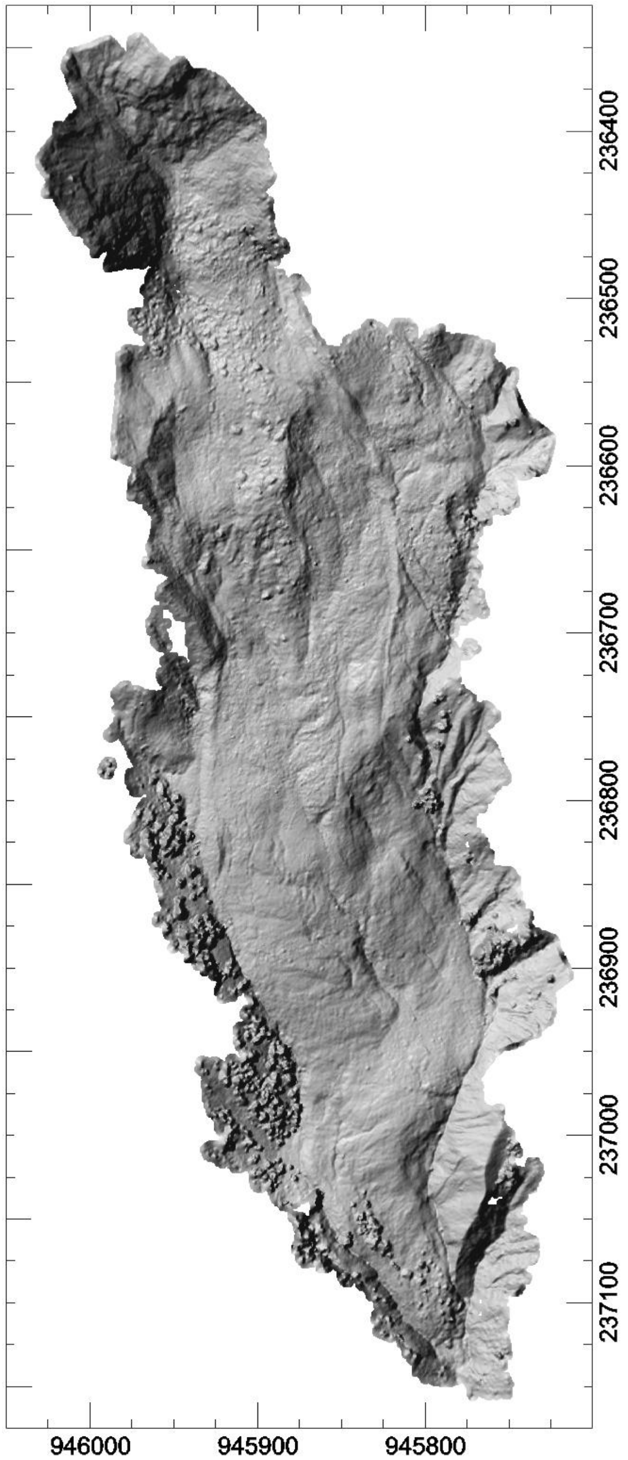


Figure 10. Hillshading of the entire landslide surface model

## 6. CONCLUSIONS

In this study it was shown that a low-cost UAV-based remote sensing approach reveals high-resolution digital surface models of landslides. The proposed structure from motion method can easily handle unordered image collections and has provided a consistent digital surface model of the Super-Sauze landslide that is consistent with results from a more traditional photogrammetric approach. This approach does not require any ground control point information and enables surface models to be generated from UAV-based remote sensing without ground-based measurements. In many cases the area of interest cannot be directly measured because of hazardous environment. The proposed approach is therefore very well suitable in the field of landslide research. The point densities of the achieved digital surface models reach up to 70 points per square meter and are comparable to a previously generated DEM using a GOTCHA region-growing algorithm (Otto and Chau, 1989). Since the proposed algorithms do not consider any ground control point information the coordinate system of the final 3D point cloud remains indeterminate and has to be aligned in a separate processing step. Here, sizable misfits of the aligned models were observed and reducing them will be the focus of further work, for example by applying a 3D surface matching algorithm in order to match the digital surface model onto stable parts of a previously acquired DEM.

## ACKNOWLEDGMENTS

We thank all colleagues from the OMIV project (Observatoire des Instabilités de Versants) for the helpful discussions and their support in the field. The authors are grateful to Jean-Philippe Malet (School and Observatory of Earth Sciences, University of Strasbourg) for providing several datasets. Our thanks also go to Eberhard Claar (Institute for Geophysics, Universität Stuttgart) who built significant components of the quad-rotor systems. The work was supported by the DFG within the project FOR 581 'Natural Slopes'.

## REFERENCES

Aber, J. S., Aber, S. W. and Pavri, F., 2002. Unmanned small-format aerial photography from kites for acquiring large scale, high-resolution, multiview-angle imagery. In: *International Archives of the Photogrammetry, Remote Sensing and Spatial Information Sciences*, Pecora 15/Land Satellite Information IV/ISPRS Commission I/FIEOS, Denver, CO, USA.

Arya, S., Mount, D. M., Netanyahu, N. S., Silverman, R., Wu, A. Y., 1998. An optimal algorithm for approximate nearest neighbor searching fixed dimensions. *Journal of the ACM*, 45(6), pp. 891–923.

Eisenbeiss, H., Lambers, K., Sauerbier, M., 2005. Photogrammetric recording of the archaeological site of Pinchango Alto (Palpa, Peru) using a mini helicopter (UAV). In: *Proc. of the 33rd CAA Conference*, Tomar, Portugal.

Fischler, M. A. and Bolles, R. C., 1981. Random sample consensus: A paradigm for model fitting with applications to image analysis and automated cartography. *Communications of the ACM*, 24(6), pp. 381–395.

Fotinopoulos, V., 2004. Balloon photogrammetry for archaeological surveys. In: *International Archives of the Photogrammetry, Remote Sensing and Spatial Information Sciences*, XX ISPRS Congress, Istanbul, Turkey, XXXV-B5, pp. 504-507.

Furukawa, Y. and Ponce, J., 2007. Accurate, dense, and robust multi-view stereopsis. In: *Conference on Computer Vision and Pattern Recognition, IEEE Computer Society*

Gomez-Lahoz, J. and Gonzalez-Aguilera, D., 2009. Recovering traditions in the digital era: the use of blimps for modelling the archaeological cultural heritage. *Journal of Archaeological Science*, 36(1), pp. 100-109.

James, M. R., Niethammer, U., Traveletti, J., 2010. Topographic reconstruction of landslide surfaces using images from an unmanned aerial vehicle. In: *ISPRS Commission V Mid Term Symposium*, Newcastle, UK.

Jütte, K., 2008. Vergleich verschiedener low-cost Luftbildaufnahmesysteme sowie Einsatz von Drohnen: Grenzen und Möglichkeiten. In: Bayerische Landesanstalt für Wald und Forstwirtschaft. Der gepixelte Wald - Fachtagung zur Forstlichen Fernerkundung.

Leprince, S., Berthier, E., Ayoub, F., Delacourt, C., Avouac, J.-P., 2008. Monitoring earth surface dynamics with optical imagery. *EOS Transactions, American Geophysical Union*, 89(1), pp. 1-2.

Lowe, D., 2004. Distinctive image features from scale-invariant keypoints. *International Journal of Computer Vision*, 60(2), pp. 91–110.

Mikrokopter, 2010. Official Mikrokopter open source quad-rotor homepage. http://www.mikrokopter.com (accessed 10 April 2010).

Malet, J. P. and Maquaire, O., 2003. Black marl earthflows mobility and long-term seasonal dynamic in southeastern France. In: *Proceedings of the International Conference on Fast Slope Movements: Prediction and Prevention for Risk Mitigation*, Picarelli L. (ed.), Bologna, *Patron Editore*, pp. 333-340.

Niethammer, U., Rothmund, S., Joswig, M., 2009. UAV-based remote sensing of the slow-moving landslide Super-Sauze. In: *Malet, J.-P., Remaître, A., Boogard, T. (Eds) Proceedings of the International Conference on Landslide Processes: from geomorpholgic mapping to dynamic modelling*, Strasbourg, *CERG Editions*, pp. 69-74.

Otto, G. P., and T. K. W. Chau (1989), Region-growing algorithm for matching of terrain images. *Image Vision Comp.*, 7, pp. 83-94.

Snavely, N., Seitz, S. M., Szeliski, R., 2008. Modeling the World from Internet Photo Collections. *International Journal of Computer Vision*, 80(2), pp. 189-210.

Przybilla, H.-J. and Wester-Ebbinghaus, W., 1979. Bildflug mit ferngelenktem Kleinflugzeug. *Bildmessung und Luftbildwesen, Zeitschrift fuer Photogrammetrie und Fernerkundung*, 47(5), pp. 137-142.

Walter, M., Niethammer, U., Rothmund, S., Joswig, M., 2009. Joint analysis of the Super-Sauze (French Alps) mudslide by nanoseismic monitoring and UAV-based remote sensing. *EAGE First Break* 27(8), pp. 75-82.